

Supporting Information

Amine Groups Covered Fullerene Derive as Electron Buffer Layers for High Performance Polymer Solar Cells.

By Zhang Zhi-Guo, Li Hui, Boyuan Qi, Dan Chi, Zhiwen Jin, Zhe Qi, Jianhui Hou, Yongfang Li*, and Jizheng, Wang**

Experimental

Synthesis: **DMAPA-C₆₀** was obtained via the *N-H* addition of alkylamines into the double bonds of fullerene as described by Wudl et al.^[14] Under the protection of argon atmosphere, a mixture of fullerene (100 mg) and 3-Dimethylaminopropylamine (5 g) in 5 ml toluene was refluxed for 12h. Volatile material was removed in vacuum, and hexane was added to wash the crude product three times. Then the residual brown solid was re-dissolved in THF and poured into 150 ml hexane to precipitate the product, which was then further purified by washing with hexane three times, and brown solid (80 mg) was obtained. Elemental analysis shows that the C/N weight ratio of 8.37 corresponds to an average of four 3-Dimethylaminopropylamine groups per C₆₀, leading to the stoichiometry of [C₆₀H₄(NHCH₂CH₂CH₂NC₂H₅)₄]. IR (KBr, cm⁻¹): 3412.7, 2939.7, 2854.5, 2813.2, 2764.7, 1656.83, 1459.8, 1402.7, 1381.6, 1264.5, 1154.7, 1040.4, 1040.45, 839.4, 765.8, and 526.5. ¹H NMR (400 MHz, CDCl₃), δ(ppm): 4.2-2.7 (br, 20H), 2.22-2.26 (br, 24H), 1.88-1.92 (br, 4H), 1.26-1.24 (br, 8H). ¹³C NMR (100 MHz, CDCl₃), δ(ppm): 155.1-140.2 (br), 58.12, 45.7, 29.8, 18.7. From the ¹H NMR spectrum, the disappearance of the NH₂ peak at 1.15 ppm together with the appearance of the NH-C₆₀ peak (3.0 ppm) and C₆₀-H (1.88-1.92 ppm) strongly support the N-H addition reaction and the proposed molecular structure

(Figure 1b). In addition, the NH-C60 peak was confirmed by heavy water exchange. In the FT-IR spectroscopy (Figure S2), the characteristic absorption peaks of pristine C60 appear at 576, 1182, and 1428 cm^{-1} . After DMAPA modification, these peaks are absent, thus confirming the idea of a multiadduct being synthesized. The appearance of bands at 1000–1200 cm^{-1} (vibrations of the C–N bond), strong bands around 2964 cm^{-1} (arising from the C–H stretching vibrations of the aliphatic portions of the molecule) confirm the covalent bonding between the amine and fullerene. In the ^{13}C NMR, the characteristic peak of pristine C60 at 143 ppm was disappeared, this characteristic peak was replaced by broad peaks at 155.1–140.2 ppm. Peaks of the alkyl at 58.2–18.67 ppm of DMAPA have emerged. Notably, the broad nature of NMR spectrum suggests that DMAPA-C60 is a mixture of components. This is consistent with the high reaction activity of this C-H addition as described by Wudl. As a result, the defined addition number can't be controlled for this type of reaction and the obtained material is a mixture of components.

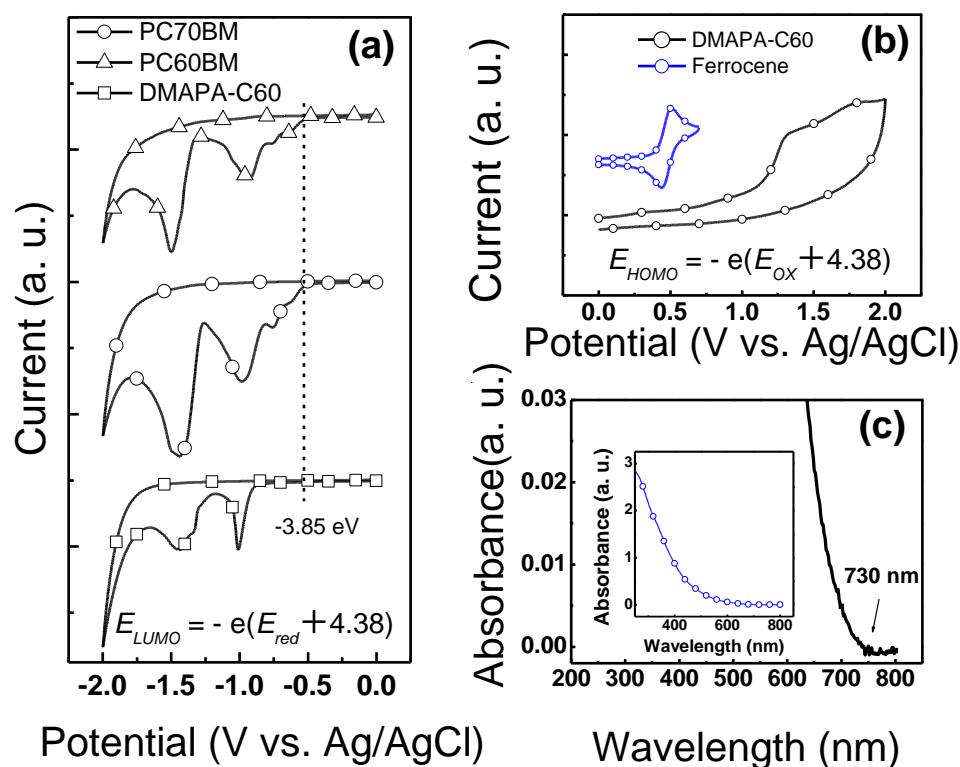


Figure S1 (a) Cyclic voltammograms of DMAEA-C₆₀, PCBM and PC₇₀BM film in a negative direction (on glassy carbon electrode in a 0.1 mol/L n-Bu₄NPF₆ acetonitrile solution at a sweep rate of 100 mV/s); (b) Cyclic voltammograms of DMAEA-C₆₀ in a positive direction (c) film absorption spectrum. The cyclic voltammogram of ferrocene was also put in inset of Figure 1b for the potential calibration.

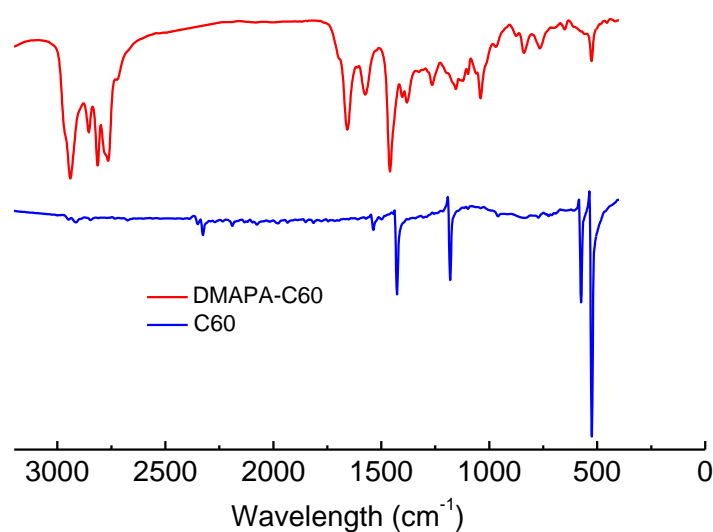


Figure S2. Comparison of the FT-IR spectra of DMAEA-C60 and C60.

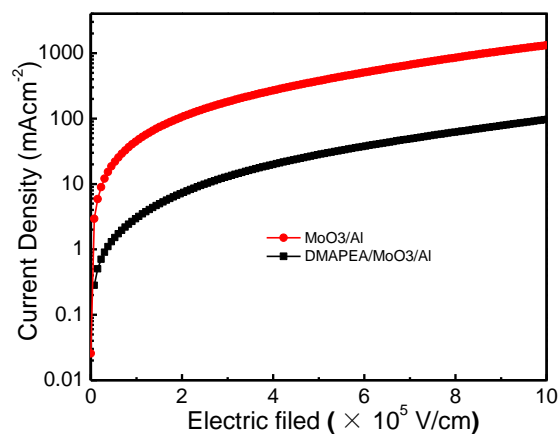


Figure S3. J-V curves of hole-only devices in the configurations of ITO/PEDOT:PSS /P3HT:PCBM (1:1 w/w, 150 nm)/ DMAEA-C60 (1mg/ml) or without DMAEA-C60 /MoO₃ (6 nm)/Al(100 nm).

Table S1. Effect of DMAEA-C60 and different cathodes on device performance of P3HT: PCBM based PSCs.

Cathode	Voc (V)	Jsc (mA•cm ⁻²)	FF (%)	PCE (%)
Ca/Al	0.625	9.01	67.47	3.80
CBL(1mg/ml)/Al	0.626	9.14	67.78	3.88
CBL(1mg/ml)/Au	0.609	8.05	61.55	3.01
CBL(1mg/ml)/Cu	0.621	9.10	65.64	3.70
CBL(1mg/ml)/Ag	0.610	8.76	56.25	3.01
Au	0.263	7.92	39.05	0.81
Al	0.435	8.38	51.83	1.89
Ag	0.428	8.47	44.41	1.60
Cu	0.372	8.23	46.47	1.42

Figure S4. Effect of DMAEA-C60 and different cathodes on device performance of PBDTTTT-C: PC70BM based PSCs.

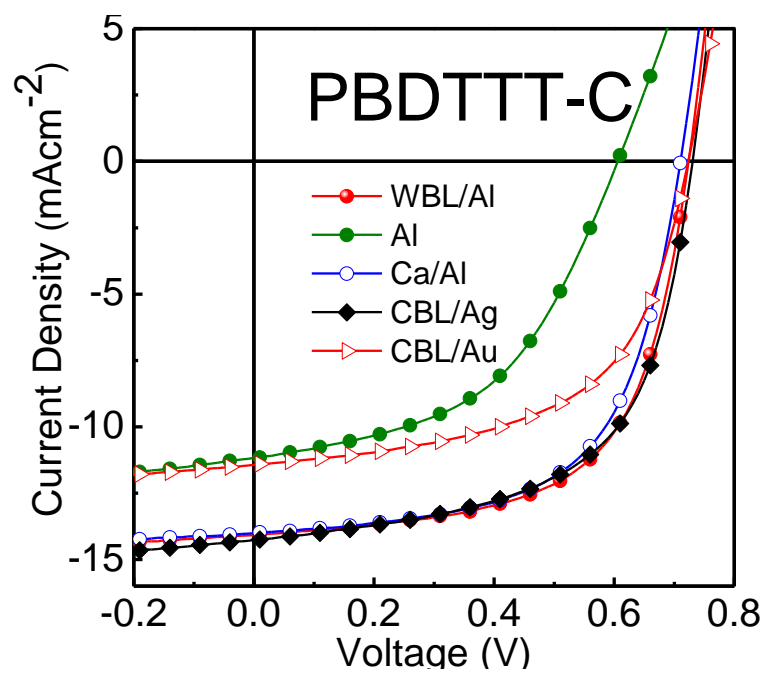


Table S2. Effect of DMAEA-C60 CBL thickness on device performance of PBDTTTT-C: PC70BM based PSCs.

Cathode	CBL (mg/ml)	V_{oc} (V)	J_{sc} (mA•cm ⁻²)	FF (%)	PCE (%)	R_s^a Ω•cm ²	R_p^b KΩ•cm ²
Al	0.5	0.726	13.80	60.19	6.03	2.22	0.57
Al	1.0	0.723	14.08	61.81	6.29	2.09	0.63
Al	1.5	0.724	13.82	56.09	5.61	3.30	0.49
Al	2.0	0.720	13.35	50.43	4.85	4.55	0.36

Figure S5. (a) Effect of DMAEA-C60 CBL thickness on device performance of PBDTTTT-C: PC70BM based PSCs. (b) R_s and R_p versus DMAEA-C60 CBL thickness.

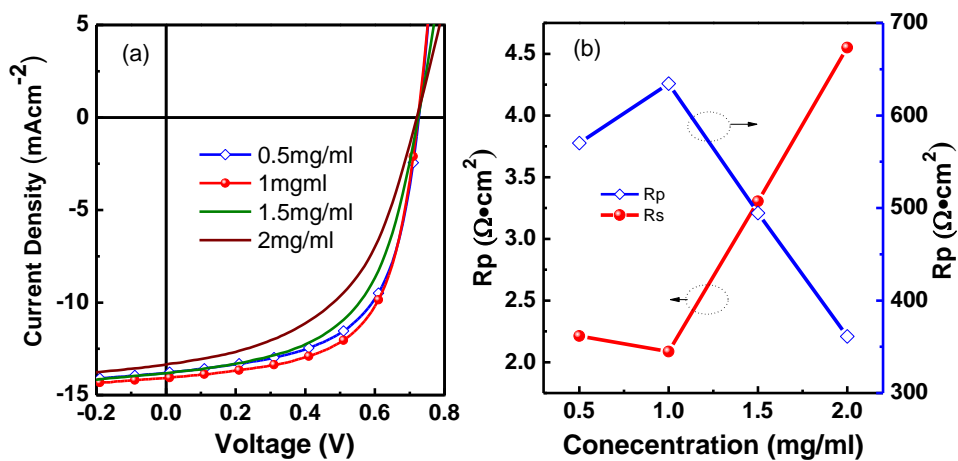


Table S3. Effect of DMAEA-C60 CBL on device performance of PBDTTTTT-C-T: PC70BM based PSCs.

Cathode	CBL (mg/ml)	V_{oc} (V)	J_{sc} (mA•cm ⁻²)	FF (%)	PCE (%)	R_s^a Ω•cm ²	R_p^b KΩ•cm ²
Al	none	0.621	12.41	53.64	4.13	2.44	0.60
Ca/Al	none	0.787	14.83	62.36	7.28	-	-
Al	0.5	0.789	14.68	60.48	7.01	2.51	0.47
Al	1.0	0.792	14.89	62.93	7.42	2.23	0.55
Al	1.5	0.792	14.23	58.60	6.60	2.84	0.45
Al	2.0	0.787	13.90	54.58	5.97	4.37	0.32

Figure S6. (a) Effect of CBL film thickness on device performance of PBDTTT-C-T: PC70BM based devices; (b) R_s and R_p versus DMAEA-C60 CBL thickness.

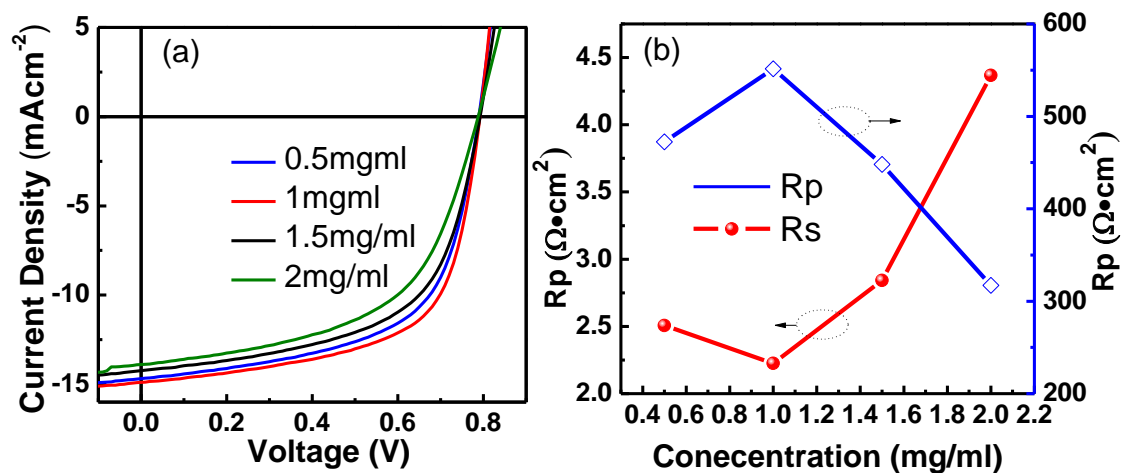


Figure S7. The dark current of P3HT: PC60BM based devices.

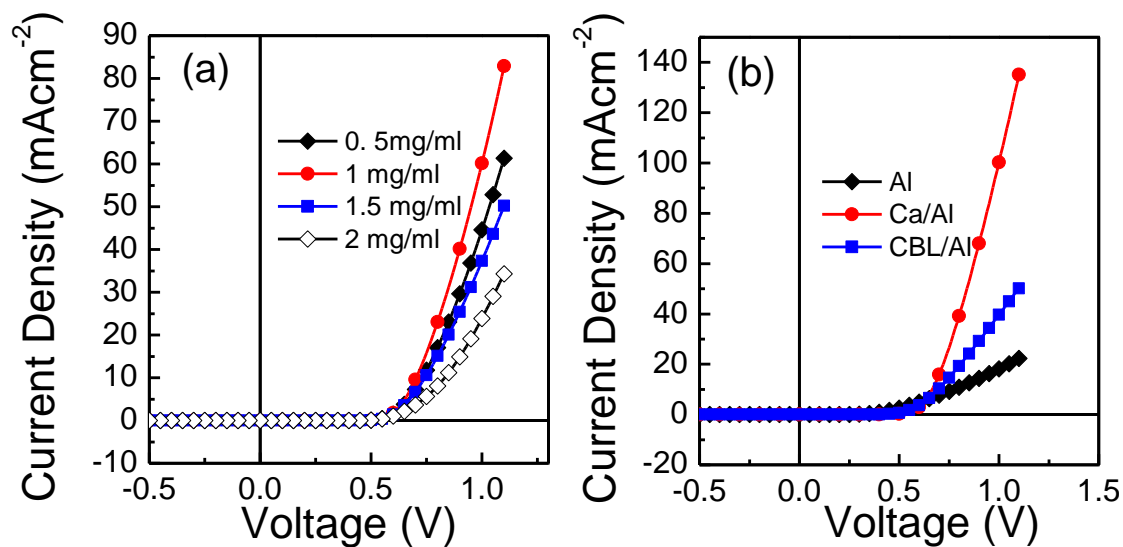
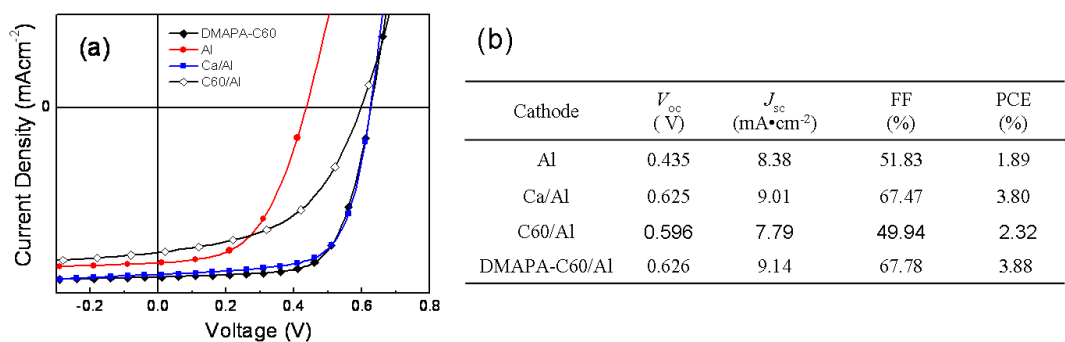
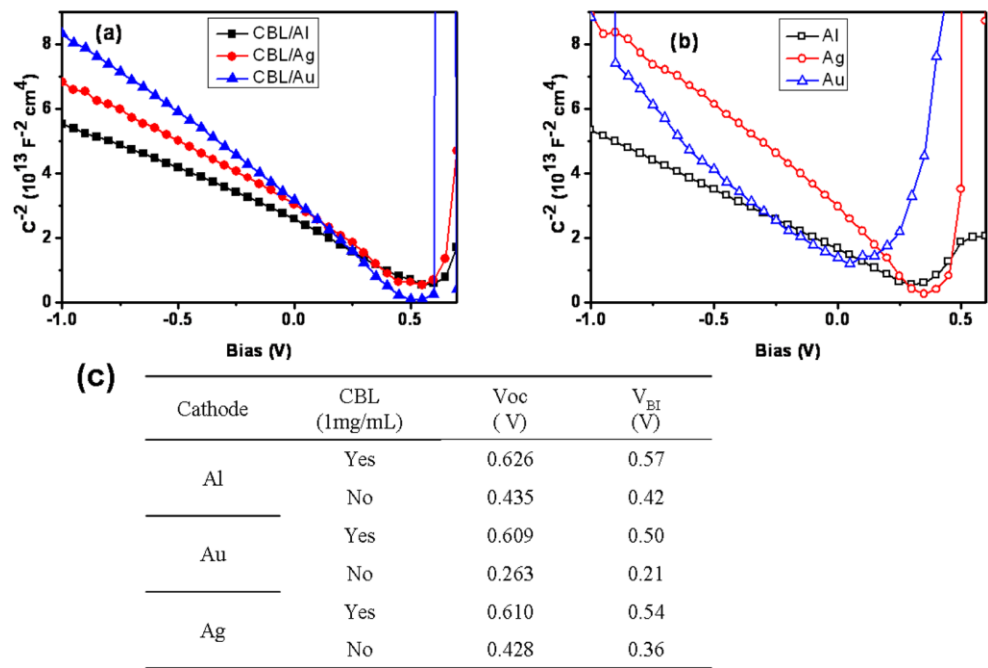


Figure S8. (a) The effect of the cathode buffer layer on P3HT: PCBM solar cell performance and (b) the summary device parameters.



The obtained V_{oc} was increased from 0.435 V for the Al only device to 0.596 V for the C60 treated device. The slightly incensement in V_{oc} is benefited from the hole blocking effect of C60 and/or the dipole moment due to the C60-Al interactions. Clearly, these two factors are not enough to provide sufficient V_{oc} as compared to the stand Ca/Al device (0.625V).

Figure S9. Mott–Schottky plots of PSCs of glass/ITO/PEDOT:PSS/P3HT:PC60BM/cathode (a) with and (b) without cathode buffer layer ($f = 100$ Hz) .(c) The summary of V_{BI} and V_{OC} values with and without cathode buffer layer.



The capacitances (C) in a range from a low-forward bias to reverse bias are related to the width of the depletion zone and estimated the depletion width (w), impurity concentration (N) that arises from structural inhomogeneities or chemical impurities present in the organic semiconductor and built-in potential (V_{BI}) of PSCs according to the Mott–Schottky model,

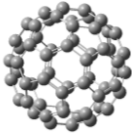
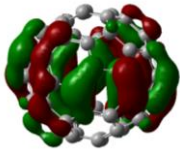
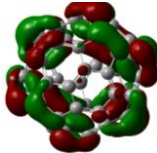
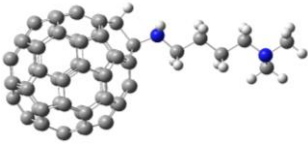
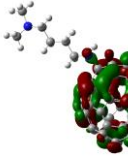
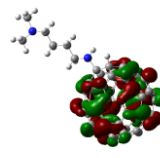
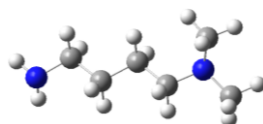
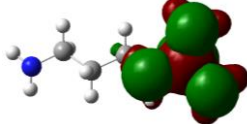
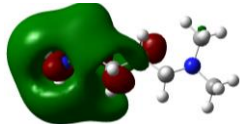
$$\frac{1}{C^2} = \frac{2}{q\epsilon_r\epsilon_0NA^2}(V_{BI} - V) \quad (1)$$

Where q is the elemental charge, ϵ_r is the relative permittivity of the organic semiconductor that is around 3, ϵ_0 is the vacuum permittivity, and A is the area of the polymer solar cell.

By extrapolating the linear portion of a curve in the low-forward bias range, the interception to x-axis yields V_{BI} of the device according to eqn (1). The V_{BI} and V_{OC} values of the devices are listed in Figure S8(c). Due to the difference in the work function of top cathodes, their corresponding devices show substantial different V_{BI} thus V_{OC} values. After CBL treatment, the devices show similar V_{BI} thus V_{OC} values. Clearly, the increase in V_{BI} and V_{OC} is caused by the increase in the work functions of the cathodes. The DMAPA-C60 buffer layer treated device produced higher built-in potential (V_{BI}). This result can explain the independence of the V_{oc} on the work function of the top cathodes.

The success of this cathode buffer layer is resulted from its multifunction: the polar group can provide dipole moment, while the fullerene moieties can provide additional hole blocking effect (suppress the carrier recombination) and enhance the conductivity (reduce R_s) of the buffer layer

Figure S10. The frontier molecular orbitals (HOMO and LUMO) and the dipole moments obtained from DFT calculations on C60, mono-additional DMAPA-C60 and DMAPA at B3LYP/6-31G* level.[1]

Models	HOMO	LUMO	Dipole moment (Deybe)
			0
			2.877
			0.844

It can be seen from Figure S10 that the DMAPA functionalized C60 can provide a much higher dipole moment (1.877 Debye) than that of DMAPA (0.844 Debye). The increment of dipole moment is resulted from the interactions between the DMAPA group and C60 group as can be seen from the frontier molecular orbital in Figure S10. Thus amine group functionalized C60 can provide a large Voc (0.626 V) than that of C60 buffer layer based device (0.596 V).

Referenece

- [1] Gaussian 03, R. E.; Frisch, M. J.; Trucks, G. W.; Schlegel, H. B.; Scuseria, G. E.; Robb, M. A.; Cheeseman, J. R.; Montgomery, J. A.; Vreven, J., T.; Kudin, K. N.; Burant, J. C.; Millam, J. M.; Iyengar, S. S.; Tomasi, J.; Barone, V.; Mennucci, B.; Cossi, M.; Scalmani, G.; Rega, N.; Petersson, G. A.; Nakatsuji, H.; Hada, M.; Ehara, M.; Toyota, K.; Fukuda, R.; Hasegawa, J.; Ishida, M.; Nakajima, T.; Honda, Y.; Kitao, O.; Nakai, H.; Klene, M.; Li, X.; Knox, J. E.; Hratchian, H. P.; Cross, J. B.; Bakken, V.; Adamo, C.; Jaramillo, J.; Gomperts, R.; Stratmann, R. E.; Yazyev, O.; Austin, A. J.; Cammi, R.; Pomelli, C.; Ochterski, J. W.; Ayala, P. Y.; Morokuma, K.; Voth, G. A.; Salvador, P.; Dannenberg, J. J.; G., Z. V.; Dapprich, S.; Daniels, A. D.; Strain, M. C.; Farkas, O.; Malick, D. K.; Rabuck, A. D.; Raghavachari, K.; Foresman, J. B.; Ortiz, J. V.; Cui, Q.; Baboul, A. G.; Clifford, S.; Cioslowski, J.; Stefanov, B. B.; Liu, G.; Liashenko, A.; Piskorz, P.; Komaromi, I.; Martin, R. L.; Fox, D. J.; Keith, T.; Al-Laham, M. A.; Peng, C. Y.; Nanayakkara, A.; Challacombe, M.; Gill, P. M. W.; Johnson, B.; Chen, W.; Wong, M. W.; Gonzalez, C.; Pople, J. A. **Gaussian, Inc., Wallingford CT, 2004.**